

**AUTHORS:**Samuel O.O. John<sup>1</sup>   
Iyabo T. Usman<sup>2</sup> **AFFILIATIONS:**<sup>1</sup>Department of Physics, Nasarawa State University, Keffi, Nigeria  
<sup>2</sup>Nuclear Structure Research Group, School of Physics, University of the Witwatersrand, Johannesburg, South Africa**CORRESPONDENCE TO:**

Samuel John

**EMAIL:**

samjoh2014@gmail.com

**DATES:****Received:** 06 Apr. 2021**Revised:** 22 Oct. 2021**Accepted:** 16 Nov. 2021**Published:** 29 Mar. 2022**HOW TO CITE:**John SOO, Usman IT. Isotopic profiling of natural uranium mined from northern Nigeria for nuclear forensic application. *S Afr J Sci.* 2022;118(3/4), Art. #10678. <https://doi.org/10.17159/sajs.2022/10678>**ARTICLE INCLUDES:**

- 
- Peer review
- 
- 
- Supplementary material

**DATA AVAILABILITY:**

- 
- Open data set
- 
- 
- All data included
- 
- 
- On request from author(s)
- 
- 
- Not available
- 
- 
- Not applicable

**EDITOR:**

Michael Inngs

**KEYWORDS:**

isotopic profile, natural uranium, U-Th-Pb concentration, nuclear forensics, uranium isotope ratio

**FUNDING:**

Petroleum Technology Development Fund



# Isotopic profiling of natural uranium mined from northern Nigeria for nuclear forensic application

Four mined samples of natural uranium from northern Nigeria were studied through inductively coupled plasma mass spectrometry, at the Environmental Analytical Chemistry Laboratory, University of the Witwatersrand, Johannesburg. The samples were characterised for lead, thorium and uranium isotopic concentrations, isotopic ratios and age. The objective was to obtain nuclear forensic fingerprints as baseline data to add to the Nigerian National Nuclear Forensic Library. Results showed significant variation in the isotopic concentrations of lead, thorium and uranium across the mines. Isotopic ratios of  $^{238}\text{U}/^{235}\text{U}$ ,  $^{235}\text{U}/^{238}\text{U}$  and  $^{234}\text{U}/^{238}\text{U}$  across the sample of  $137.881 \pm 0.007$ ,  $7.253 \times 10^{-03} \pm 2.05 \times 10^{-04}$  and  $5.540 \times 10^{-05} \pm 4.08 \times 10^{-07}$  were found to be consistent with the natural values. The age of natural uranium is comparable to the age of earth. Uranium, lead, and thorium isotopic concentrations and ratios, as well as the age of the samples characterised, provide an isotopic profile that can be used for nuclear forensic application.

**Significance:**

- Given the abundant deposits of natural uranium in Africa and the consequent potential for nuclear insecurity, determining the isotopic profiles and signatures of natural uranium is important for application in nuclear forensics.
- Isotopic concentrations of  $^{232}\text{Th}$ ,  $^{238}\text{U}$ ,  $^{235}\text{U}$  and  $^{234}\text{U}$  from the respective sampling sites differed significantly, thereby providing characteristic isotopic profiles.

## Introduction

Nuclear forensics operates on the premise that some measurable parameters in nuclear materials provide signatures according to their geological origin for identification purpose.<sup>1-3</sup> Nuclear forensics is the examination of nuclear or other radioactive material, or of evidence that is contaminated with radionuclides, in the context of legal proceedings under international or national law related to nuclear security. The analysis of nuclear or other radioactive material seeks to identify what the materials are, how, when, and where the materials were made, and what their intended uses were.<sup>2,4</sup> Successful studies have been reported across the globe on many samples of materials that are nuclear and radioactive in nature, yielding signatures such as uranium isotopic compositions and ratios, and impurities of elements such as lanthanides (rare earth elements), lead (Pb), strontium (Sr), sulfur (S) and neodymium (Nd).<sup>5-9</sup> However, data on Africa – a continent that is well endowed with natural uranium – are still scarce; hence, the present study is pertinent.<sup>10</sup>

Natural uranium, which is radioactive, is mined and processed to obtain uranium ore concentrate or yellowcake, which is further transformed into nuclear fuel elements, used in research reactors and power reactors for electricity generation.<sup>2,11</sup> The database of the International Atomic Energy Agency on unlawful trafficking<sup>12</sup> includes many events of peddling in inferior nuclear materials containing natural uranium. For instance, in recent years, 400 of 3068 incidents involving depleted, natural or low-enriched uranium, were included in the Incident and Trafficking Database of the International Atomic Energy Agency, through the application of nuclear forensic science.<sup>2,4,12</sup> Keegan et al.<sup>13</sup> reported a small glass jar labelled 'Gamma Source' discovered by police in a clandestine drug laboratory in Australia, 2009. After extensive nuclear forensic analysis of the material, Keegan et al.<sup>13</sup> found it to be most likely from Mary Kathleen, a defunct Australian uranium mine. Nuclear forensic science is used to characterise various uranium samples and obtain nuclear fingerprints to enable the tracing of their origins.

The isotope system of uranium is special: of its 25 known isotopes which have a mass range of 217–241u<sup>6</sup>, only  $^{238}\text{U}$  ( $t_{1/2} = 4.468 \times 10^9$  y; 99.274%),  $^{235}\text{U}$  ( $t_{1/2} = 7.038 \times 10^8$  y; 0.7204%) and  $^{234}\text{U}$  ( $t_{1/2} = 2.455 \times 10^5$  y; 0.00548%) are naturally occurring at significant concentrations.<sup>7,14,15</sup> The decay series nuclides of uranium and thorium have characteristics and chemical affinities applicable to a wide range of processes.<sup>1,4,16</sup> They have half-lives that are proportional to their equilibrium abundances, while the short-lived progenies exhibit low concentrations with very great isotope ratios.<sup>16</sup> For instance, the concentrations of  $^{232}\text{Th}$  and  $^{238}\text{U}$  are available in ppb to ppm while those of  $^{234}\text{U}$  and  $^{236}\text{U}$  can be as low as ppt for ores of granitic origin.<sup>2,17,18</sup>

The natural compositions, concentrations and ratios of uranium, thorium and lead isotopes have proved to be viable signatures in nuclear forensics.<sup>3,8</sup> In addition, when the isotopic ratios  $^{234}\text{U}/^{238}\text{U}$  and  $^{235}\text{U}/^{238}\text{U}$  are simultaneously analysed, nuclear and radioactive materials that contain uranium from various geological origins can be distinguished.<sup>19-21</sup> Until very recently, there was an assumption that the isotopic ratios  $^{235}\text{U}/^{238}\text{U}$  and  $^{234}\text{U}/^{238}\text{U}$  of terrestrial materials are constant ( $7.25 \times 10^{-5}$  and  $5.48 \times 10^{-7}$ , respectively). However, using modern analytical procedures, the ratios now show variations in different geological materials of 1.3%.<sup>2,7,13,22</sup> Recent nuclear forensic investigations on natural uranium and uranium ore concentrate samples showed that uranium isotopic compositions, isotopic ratios and age, among other parameters, are key nuclear forensic signatures that can be used to identify materials.<sup>3,10,23</sup> Bopp et al.<sup>24</sup> studied uranium samples from both low- and high-temperature deposits and concluded that during the low-temperature redox transition,  $^{238}\text{U}/^{235}\text{U}$  fractionation occurred, which is the phase transition of isotopes from a lighter to heavier isotope, which results in higher ratio values. Brennecke et al.<sup>7</sup>, on the other hand, studied  $^{235}\text{U}/^{238}\text{U}$  ratios of uranium ore concentrate samples in order to relate observed

variations in  $^{238}\text{U}/^{235}\text{U}$  to the U mineralisation mechanism in the main ore. They found that  $^{235}\text{U}/^{238}\text{U}$  fractionation occurred following redox transformation of uranium from U(VI) to U(IV) at low temperature, giving uranium ore concentrates originating from low-temperature redox type deposits a unique  $^{235}\text{U}/^{238}\text{U}$  ratio.

We used a modern analytical (destructive) technique, inductively coupled plasma mass spectrometry (ICP-MS), to measure and establish the isotopic profiles of samples of natural uranium from the northern part of Nigeria. Our aim was to obtain baseline data for application in the area of nuclear forensic science.

## Materials and methods

### Study site and investigated samples

Four open pit samples of natural uranium in rock form were investigated. The vein-type, high-temperature magmatic, granite-related uranium deposit<sup>25,26</sup> samples were collected from the northern part of Nigeria (Figure 1). The samples were collected according to the uranium ore sample collection standard at the following uranium mining sites: Riruwai (a pyrochlore in peralkaline granite uranium of average grade 540 ppm), Mika (two locations – Mika-I and Mika-II – of pitchblende-rhyolite mineralisation of grade 215 ppm) and Michika (brecciated, silicified and mylonitised rocks of average grade 2000 ppm). The sample sites were chosen based on their geology and mineralisation, following previous prospecting of uranium in the sampling locations.<sup>27-33</sup> About 2 kg of natural uranium rock samples, obtained by means of chisel and mallet, from each pit mine site, were placed in a zip-locked plastic bag to avoid contamination. The samples were collected between 11 February and 3 March 2018, at a depth ranging from 1.3 m to 5.9 m. The collected samples were then kept in a safe location for a short time and transferred to the Environmental Analytical Chemistry Laboratory (University of the Witwatersrand, Johannesburg, South Africa) for measurement and analysis.

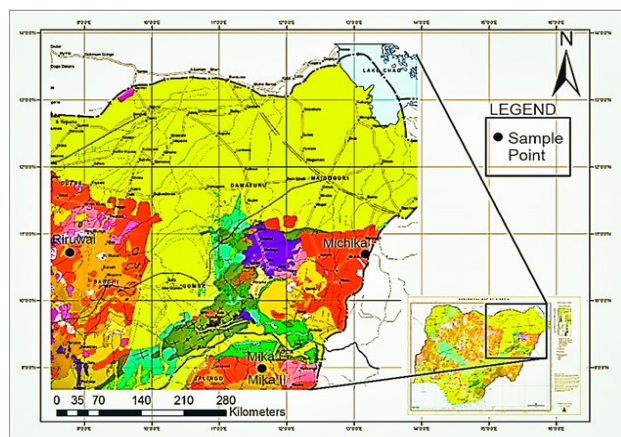


Figure 1: Map of Nigeria showing the uranium mining sites where samples for this work were collected.

### Instrumentation and measurement

#### Sample preparation for ICP-MS

The ICP-MS analytical method requires that samples for measurement be presented in liquid form or as an aerosol matrix. The rock crusher and milling devices located at the Geosciences Laboratory (University of the Witwatersrand), were used to process the natural uranium samples into a soluble fine powder.

A digital microwave digestive device was used to dissolve the milled natural uranium samples under conditions of high pressure and temperature. Microwave preparation of samples under such conditions presents benefits such as complete sample dissolution using hydrofluoric and nitric acids. It also improves detection limits due to

the use of a lower sample to solution ratio and prevents volatilisation of certain elements through use of high pressure.

A quick test for the presence of silica was done, as silica can form precipitate during sample preparation and tends to absorb the elements, making it difficult for their detection by ICP-MS. Silica can also affect the nebuliser, by making it difficult for the sample to get into the plasma for the process of isotope measurement. The milled samples (~0.5 g each) were placed in Teflon heating containers. Concentrated solutions of  $\text{HNO}_3$  and  $\text{HCl}$  in volumes of 1.0 mL and 4.0 mL, respectively, were added followed by  $\text{H}_2\text{O}_2$  in drops to a volume of 0.5 mL. After sample pre-digestion, each container was tightly sealed and placed on a rotor in the microwave. The microwave unit was set to a method ASTM D4 309 (half-scale): 4 vessels, 9.0 mL sample per vessel with a temperature of  $180^\circ\text{C}$  and 90% (10.13 kPa) pressure then powered-on for a maximum period of 50 min. The cooled digested sample solutions appeared to be very clear without silica precipitate, implying that silicates were not present in the samples in a quantity that required further action using hydrofluoric acid to remove the silicate.

#### ICP-MS analysis

An ICP-MS device (Agilent 7700, Agilent Technologies, Inc., Santa Clara, CA, USA), was used to analyse the samples. Table 1 presents the summary of the set-up parameters for optimised equipment usage.

Table 1: Set-up parameters for the inductively coupled plasma mass spectrometry device used in natural uranium sample analysis

Parameter	Value
Radiofrequency forward and reflected power	1550 W; 14 W
Plasma mode and gas flow	Normal, robust; 1000 mL/min
Flow rate of auxiliary gas	1000 mL/min
Flow of carrier gas and pressure	1000 mL/min; 740.5 kPa
Sampling depth	8 mm
Cones	Nickel
Cell gas	Argon
Spray chamber temperature	$2.0^\circ\text{C}$
Type of detector value	Dual mode
Integration time	100 $\mu\text{s}$
Replicate per sample	2
Mode	Collision mode

Both the prepared and blank samples, the calibration standards (5 ppb, 20 ppb, 50 ppb, 100 ppb, 500 ppb, and 1000 ppb) with samples for quality control (20 ppb and 100 ppb) were all put into the auto-sampler for ICP-MS analysis. The tubes of the device were cleaned using a nitric acid solution to avoid washing of residual memory, usually done before placement of samples in the device. The tubing cleaning process was repeated after each sample measurement, to avoid cross-contamination. The process is automatic and computerised. The control was performed on the computer system via installed software (ICP-MS MassHunter Workstation for running Agilent 7700 series). The analysis produced results for various isotopes, which were then analysed further. Additional details of the experimental analysis can be found in John et al.<sup>33</sup>

## Results

### Uranium isotopic concentration

Concentrations of  $^{238}\text{U}$  and  $^{232}\text{Th}$ , which are the most stable and abundant of the isotopes, were obtained through ICP-MS analysis. As the isotopic

**Table 2:** Measured and determined isotopic concentrations of thorium and uranium

Sample location	<sup>232</sup> Th (ppm)	<sup>238</sup> U (ppm)	<sup>235</sup> U (ppm)	<sup>234</sup> U ( $\times 10^{-05}$ ) (ppm)
Riruwai	5.410 ± 0.318	1.318 ± 0.049	0.009 ± 0.0001	0.053 ± 2.0 $\times 10^{-08}$
Mika-I	0.055 ± 0.006	0.084 ± 0.003	0.001 ± 1.9 $\times 10^{-05}$	0.0034 ± 1.0 $\times 10^{-09}$
Mika-II	0.159 ± 0.003	73.965 ± 1.371	0.536 ± 0.009	2.972 ± 5.5 $\times 10^{-07}$
Michika	0.061 ± 0.002	7.854 ± 0.293	0.057 ± 0.002	0.316 ± 1.2 $\times 10^{-07}$

concentration of uranium in nature is constant (the relative percentages being 99.2745%, 0.7204% and 0.00548% for <sup>238</sup>U, <sup>235</sup>U and <sup>234</sup>U, respectively), isotopes <sup>235</sup>U and <sup>234</sup>U were determined by Equation 1<sup>15,34</sup>:

$$C_{235U} = \frac{0.7200}{99.2745} \times C_{238U}, \quad \text{Equation 1}$$

where and are the respective concentrations of isotopes <sup>235</sup>U and <sup>238</sup>U. In the same way, the value for isotope <sup>234</sup>U was obtained where isotope <sup>235</sup>U was replaced by <sup>234</sup>U alongside the value of its percentage composition.

A summary of the results of uranium and thorium concentrations for the various locations is presented in Table 2. From these results, the concentration range of <sup>232</sup>Th for the entire samples, 0.055±0.006 to 5.410±0.318 ppm, was below the average crustal concentration range for <sup>232</sup>Th, which is 8–12 ppm.<sup>35</sup>

Two concentrations obtained for the uranium isotopes were lower than the average crustal concentration (2–3 ppm <sup>238</sup>U): Riruwai (1.318±0.049 ppm) and Mika-I (0.084±0.003 ppm). However, the concentration of uranium isotopes from Mika-II (73.965±1.371 ppm) was far higher than the world average, while that for Michika (7.854±0.293 ppm) was close to the world average.

<sup>235</sup>U and <sup>234</sup>U concentration ranges across the sample locations were 0.001±1.9 $\times 10^{-5}$  ppm to 0.536±0.009 ppm and 3.384 $\times 10^{-8}$ ±1.0 $\times 10^{-9}$  ppm to 2.972 $\times 10^{-5}$ ±5.5 $\times 10^{-7}$  ppm, respectively. Lower and higher concentrations obtained were both from Mika-I and Mika-II. Possible factors contributing to errors in values reported in this study could be sample inhomogeneity, uncertainty calculations with respect to uranium isotope composition, and uncertainty of weighing. However, due to the method used – ICP-MS involving isotope dilution or calibration curve – uncertainty was reduced to the lowest possible.

Figure 2 presents the variable isotopic concentration of radiogenic lead in this study. Its presence in samples in differing amounts from both primordial and radiogenic lead depends on geological age and uranium/thorium content. The Riruwai sample had the highest concentration of radiogenic lead while the Michika sample had the lowest. A range of 0.004±0.001 ppm to 4.447±0.322 ppm was found for all the samples. These measured lead isotope values were further used to determine the age of the samples.

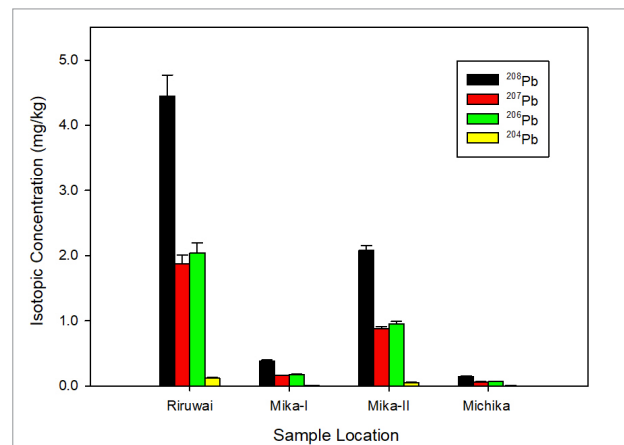


**Figure 2:** Lead (Pb) isotopic concentration (mg/kg or ppm) of samples obtained from the four study sites.

### Isotopic concentration ratio

The natural isotopic ratio and variation of uranium and thorium is a characteristic profile used to trace the origin of a uranium-bearing material.<sup>2,13</sup> The isotopic ratios considered in this study were <sup>238</sup>U/<sup>235</sup>U and <sup>235</sup>U/<sup>234</sup>U together with <sup>235</sup>U/<sup>238</sup>U and <sup>234</sup>U/<sup>238</sup>U. The <sup>232</sup>Th/<sup>238</sup>U isotopic ratio was also determined.

The isotopic ratios <sup>238</sup>U/<sup>235</sup>U, <sup>235</sup>U/<sup>234</sup>U, <sup>235</sup>U/<sup>238</sup>U together with <sup>234</sup>U/<sup>238</sup>U were determined from concentration values (ppm) measured by ICP-MS and are presented in Table 3. The <sup>238</sup>U/<sup>235</sup>U isotopic ratio obtained in this study is 137.881±0.007 and it shows no significant variation across the sample locations, but equals the constant value for natural uranium under the solar system, which is 137.88.<sup>22,36,37</sup> The <sup>235</sup>U/<sup>234</sup>U isotopic ratio yielded a value of 130.911±0.290, and also shows no significant variation across the samples, but is comparable with that reported by Brenneka et al.<sup>7</sup> within the world's range value of 83.63–164.17, from different geochemical environments. The standard value for the isotopic ratios <sup>235</sup>U/<sup>238</sup>U and <sup>234</sup>U/<sup>238</sup>U and their variability are well known as 7.253 $\times 10^{-3}$  and 5.502 $\times 10^{-5}$ , respectively.<sup>6,38</sup> The values determined in this study are 7.253 $\times 10^{-3}$ ±2.05 $\times 10^{-4}$  and 5.540 $\times 10^{-5}$ ±4.08 $\times 10^{-7}$ , which are identical to the standard values, although there was no significant variation across the sample locations. The data on uranium isotopic ratios <sup>238</sup>U/<sup>235</sup>U and <sup>235</sup>U/<sup>234</sup>U from this study were compared with those from other parts of the world, as illustrated in Figure 3a and 3b; they were found to be consistent and comparable with the reported values.<sup>7,13,38,39</sup>

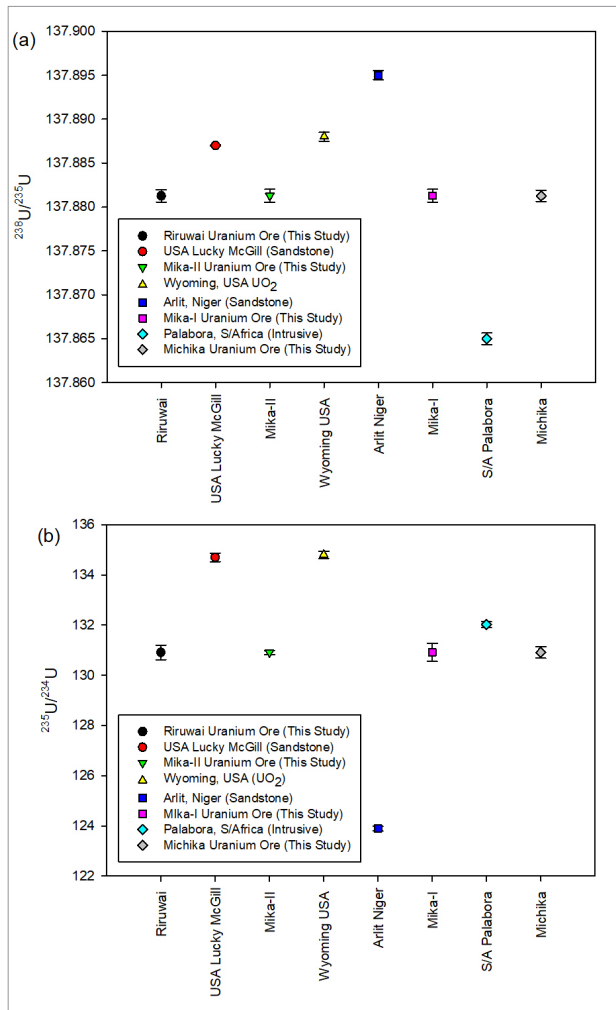


**Figure 3:** Comparison of uranium isotopic ratios (a)  $^{238}\text{U}/^{235}\text{U}$  and (b)  $^{235}\text{U}/^{234}\text{U}$  from our study sites and other parts of the world.

### Uranium age determination

Daughter-parent isotopic ratios ( $^{206}\text{Pb}/^{238}\text{U}$ ,  $^{207}\text{Pb}/^{235}\text{U}$  and Pb-Pb) were used to determine the age of natural uranium samples in units of mega-annum (Ma). Table 4 presents values of the ratios  $^{206}\text{Pb}/^{238}\text{U}$ ,  $^{207}\text{Pb}/^{235}\text{U}$  and average age determined. Table 4 shows variable ranges of  $0.008 \pm 0.002$  Ma to  $2.095 \pm 0.375$  Ma for  $^{206}\text{Pb}/^{238}\text{U}$ ,  $0.0105 \pm 0.003$  Ma to  $2.653 \pm 0.271$  Ma for  $^{207}\text{Pb}/^{235}\text{U}$  and  $29.4 \pm 0.009$  Ma to  $4280 \pm 0.046$  Ma for average age. The equation for the law of basic radioactive decay and its derivative, Equation 2, were used to determine the age of natural uranium material<sup>40-42</sup>:

$$t = \frac{(1 - \frac{R}{K})}{\beta}, \tag{Equation 2}$$

where  $t$  is the time or age of  $^{206}\text{Pb}/^{238}\text{U}$  and  $^{207}\text{Pb}/^{235}\text{U}$ ,  $R$  is the isotopic ratio of daughter-parent ( $^{206}\text{Pb}/^{238}\text{U}$  and  $^{207}\text{Pb}/^{235}\text{U}$ ),  $\beta$  is the factor that is composed of decay constants of the daughter-parent nuclei and  $K$  is the isotopic decay ratio.

**Table 4:** U-Pb isotopic ratio and average age of measured natural uranium samples

Sample location	$^{206}\text{Pb}/^{238}\text{U}$	$^{207}\text{Pb}/^{235}\text{U}$	Age (Ma)
Riruwai	$1.552 \pm 0.332$	$1.962 \pm 0.076$	$3550 \pm 0.021$
Mika-I	$2.095 \pm 0.375$	$2.653 \pm 0.271$	$4280 \pm 0.046$
Mika-II	$0.013 \pm 0.027$	$0.016 \pm 0.026$	$49.3 \pm 0.005$
Michika	$0.008 \pm 0.002$	$0.0105 \pm 0.003$	$29.4 \pm 0.009$

From the results, Mika-I has an age of  $4280 \pm 0.046$  Ma, as for younger granite, while Michika has an age of  $29.4 \pm 0.009$  Ma and is the youngest, yielding an age difference of  $4250.6 \pm 0.038$  Ma. The mean age of all the samples was  $1978.2 \pm 0.019$  Ma. The age of natural uranium is a reflection of the presence of radiogenic lead:  $^{206}\text{Pb}/^{238}\text{U}$  isotopic ratio and age of material are significantly correlated, with a correlation coefficient of 0.997 and a  $p$ -value of 0.00286. In addition, Figure 4a shows a regression curve fit with  $R^2 = 0.9998$ , implying that there was a significant correlation between the variables, which was not by chance. Hence, the variation in the age of the investigated natural uranium samples with half-lives of  $t_{1/2} \approx 4500$  Ma of  $^{238}\text{U}$  and  $t_{1/2} \approx 704$  Ma of  $^{235}\text{U}$ , shows that some fractionation occurred over the period. In addition, a negative correlation was observed between uranium concentration and age of the material. Mika-I and Mika-II samples showed an age difference of  $4230.7 \pm 0.062$  Ma due to the differences in mineralisation, geochemical formation, homogeneity of rock and concentration from the strong correlation of U-Pb in materials as well as possible error from determination of the isotopic ratio. In addition, Figure 4b–d shows the U-Pb discordia and Pb-Pb isochron for the four investigated samples.

### Discussion

Characterisation of natural uranium to obtain isotopic profiles and signatures for nuclear forensic application in support of nuclear security, safeguards and non-proliferation, is increasingly becoming important and of global interest.<sup>2</sup> Given the abundant deposits of natural uranium in Africa and the consequent potential for nuclear insecurity, providing isotopic profiles and signatures of natural uranium, especially its nuclear content, isotopic ratio and age, has application in nuclear forensics, by providing a database for reference.

**Table 3:** Uranium concentration isotopic ratios of the natural uranium samples

Sample location	$^{238}\text{U}/^{235}\text{U}$	$^{235}\text{U}/^{234}\text{U}$	$^{238}\text{U}/^{238}\text{U}$	$^{234}\text{U}/^{238}\text{U}$
Riruwai	$137.881 \pm 0.007$	$130.911 \pm 0.290$	$7.253 \times 10^{-03} \pm 2.05 \times 10^{-04}$	$5.540 \times 10^{-05} \pm 4.08 \times 10^{-07}$
Mika-I	$137.881 \pm 0.075$	$130.911 \pm 0.086$	$7.253 \times 10^{-03} \pm 6.33 \times 10^{-04}$	$5.540 \times 10^{-05} \pm 3.33 \times 10^{-07}$
Mika-II	$137.881 \pm 0.008$	$130.911 \pm 0.360$	$7.253 \times 10^{-03} \pm 6.56 \times 10^{-04}$	$5.540 \times 10^{-05} \pm 4.01 \times 10^{-07}$
Michika	$137.881 \pm 0.006$	$130.911 \pm 0.228$	$7.253 \times 10^{-03} \pm 6.83 \times 10^{-04}$	$5.540 \times 10^{-05} \pm 4.15 \times 10^{-07}$

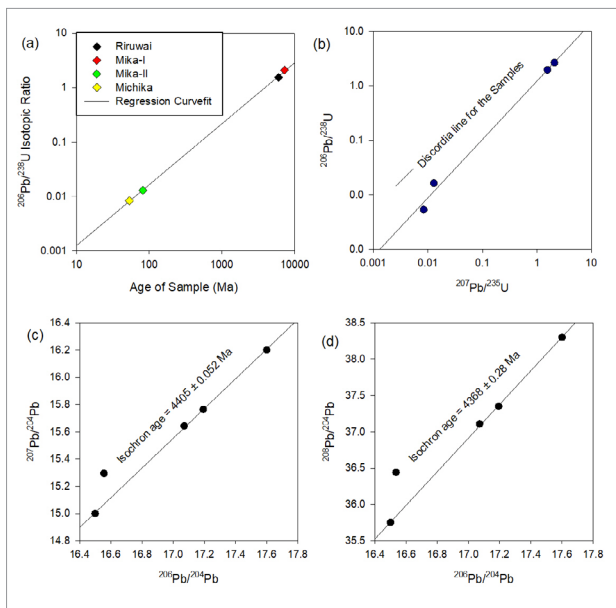


**Figure 4:** (a) A regression curve fit for the correlation of the  $^{206}\text{Pb}/^{238}\text{U}$  isotopic ratio with determined age of the natural uranium samples. (b) U-Pb discordia graph for the parent-daughter isotopic ratios ( $^{206}\text{Pb}/^{238}\text{U}$  and  $^{207}\text{Pb}/^{235}\text{U}$ ) of the samples. (c) Pb-Pb isochron diagram (for the  $^{207}\text{Pb}/^{204}\text{Pb}$  and  $^{206}\text{Pb}/^{204}\text{Pb}$  isotopic ratios) defining an isochron of  $4405 \pm 0.052$  Ma for the four samples of natural uranium from northern Nigeria. (d) Pb-Pb isochron diagram (for the  $^{208}\text{Pb}/^{204}\text{Pb}$  and  $^{206}\text{Pb}/^{204}\text{Pb}$  isotopic ratios) defining an isochron of  $4368 \pm 0.027$  Ma for the four samples of natural uranium from northern Nigeria.

The concentration ranges of uranium and thorium at various sites were below the crustal values, except at Mika-II and Michika. This, therefore, forms the basis for identifying the samples as having concentration values lower than the average crustal concentration in ppm. The high and low concentration values of the radioactive elements (uranium and thorium) in natural uranium samples measured are comparable with those reported previously.<sup>8,34,36</sup> Only small amounts of  $^{204}\text{Pb}$  were present in all the samples, as shown in Figure 2 – an indication of minerals rich in uranium/thorium.

Comparison of the data in Table 3 and Figure 3 for the uranium isotopic ratios  $^{238}\text{U}/^{235}\text{U}$  and  $^{235}\text{U}/^{234}\text{U}$  for the four samples gave a correlation coefficient of -0.775 and  $p$ -value of 0.225, implying that there is no significant relationship between any pair of the ratios. There was no significant difference between the various sample locations. Isotope concentration ratio of  $^{235}\text{U}/^{238}\text{U}$  together with  $^{234}\text{U}/^{238}\text{U}$  showed no significant variation across the various mines, with a correlation coefficient of -0.829 and  $p$ -value of 0.171 implying that there is no significant relationship between any pair of the isotope ratios. Thus, the invariant uranium isotopic ratios determined in this study can serve as supplementary information to characterise the natural uranium found in the study area.

In the decay series U-Th-Pb, analysis of daughter-parent isotopic ratios of  $^{206}\text{Pb}/^{238}\text{U}$ ,  $^{207}\text{Pb}/^{235}\text{U}$  and  $^{232}\text{Th}/^{208}\text{Pb}$  alongside the Pb-Pb isochron is useful in determining the fingerprint and age of uranium-bearing material. The parameters were measured and determined in this study. The actual  $^{235}\text{U}/^{238}\text{U}$ ,  $^{206}\text{Pb}/^{238}\text{U}$  and  $^{232}\text{Th}/^{208}\text{Pb}$  ratios present at the time of formation of the geological structure of the ore when uranium and thorium were fastened into the mineral deposit, indicate the presence of radiogenic isotopic vector. Hence, some geological age information of the deposit can be determined through isotopic composition of the decay-generated lead. The isotope system of  $^{206}\text{Pb}/^{238}\text{U}$ ,  $^{207}\text{Pb}/^{235}\text{U}$  and Pb-Pb were used in this study, considering the decay system  $^{238}\text{U} \rightarrow ^{206}\text{Pb}$ ,  $^{235}\text{U} \rightarrow ^{207}\text{Pb}$  and  $^{232}\text{Th} \rightarrow ^{208}\text{Pb}$  plays a key role in long- and short-range chronometers. Ages of the samples in this study are comparable

to the age of the earth,  $4543 \text{ Ma}^{43}$ , determined through radioactive decay chronometry and other related studies<sup>44,45</sup>. The Pb-Pb isochron (Figure 4c and 4d) presents a compatible age value to that of the earth, which correlates well with other U-Pb methods used. The highest age (of the Mika-I sample) was less than the age of the earth by 263 Ma, while the lowest age (of Michika) differed by 4513.6 Ma. The age variation, therefore, presents a unique signature for the sample in this study, which is relevant for nuclear forensic applications.

## Conclusion

Based on the results of the investigation, isotopic concentrations of  $^{232}\text{Th}$ ,  $^{238}\text{U}$ ,  $^{235}\text{U}$  and  $^{234}\text{U}$  for the respective mine sites differ significantly, thereby forming characteristic isotopic profiles of the samples. The isotopic ratios  $^{206}\text{Pb}/^{238}\text{U}$  and  $^{207}\text{Pb}/^{235}\text{U}$  show distinct variation across the mines and hence form part of the fingerprint. Other isotopic concentration ratios  $^{238}\text{U}/^{235}\text{U}$ ,  $^{235}\text{U}/^{234}\text{U}$ ,  $^{235}\text{U}/^{238}\text{U}$  and  $^{234}\text{U}/^{238}\text{U}$  were invariant for the respective mines. Perhaps, partly because concentrations of  $^{235}\text{U}$  and  $^{234}\text{U}$  isotopes were determined from  $^{238}\text{U}$  and were not measured directly, ICP-MS is not precise enough to measure the small differences in the isotopic ratios, thereby yielding concentration values that produced no significant variations. However, their values are identical and comparable to global standards and other related works, thus providing supplementary isotopic profile information to characterise the materials.

Using the isotopic ratios  $^{206}\text{Pb}/^{238}\text{U}$ ,  $^{206}\text{Pb}/^{238}\text{U}$  and Pb-Pb isochron, ages of the samples were determined and showed significant variation for the mining sites under investigation. Sample age was, therefore, a unique isotopic profile for nuclear forensic application. The very good correlation observed between isotopic ratio  $^{206}\text{Pb}/^{238}\text{U}$  and age shows the occurrence of fractionate directly related to vein-type granite mineralogy. Therefore, the samples studied can be identified by their  $^{232}\text{Th}$ ,  $^{238}\text{U}$ ,  $^{235}\text{U}$  and  $^{234}\text{U}$  isotopic concentrations and ratios  $^{206}\text{Pb}/^{238}\text{U}$ ,  $^{207}\text{Pb}/^{235}\text{U}$ , as well as age.

## Acknowledgements

We acknowledge the Nigerian Petroleum Technology Development Fund PHD-LSS Scholarship Scheme.

## Competing interests

We have no competing interests to declare.

## Authors' contributions

S.O.O.J.: Data collection, data analysis, writing. I.T.U.: Conceptualisation, methodology, student supervision.

## References

- Schwerdt IJ, Brenkmann A, Martinson S, Albrecht BD, Heffernan S, Klosterman MR, et al. Nuclear proliferomics: A new field of study to identify signatures of nuclear materials as demonstrated on alpha- $\text{UO}_2$ . *Talanta*. 2018;186:433–444. <https://doi.org/10.1016/j.talanta.2018.04.092>
- Kristo MJ, Gaffney AM, Marks N, Knight K, Cassata WS, Hutcheon ID. Nuclear forensic science: Analysis of nuclear material out of regulatory control. *Annu Rev Earth Planet Sci*. 2016;44:555–579. <https://doi.org/10.1146/annurev-earth-060115-012309>
- Mayer K, Wallenius M, Lützenkirchen K, Galy J, Varga Z, Erdmann N, et al. Nuclear forensics: A methodology applicable to nuclear security and to non-proliferation. *J Phys Conf Ser*. 2011;312(062003):1–9. <https://doi.org/10.1088/1742-6596/312/6/062003>
- International Atomic Energy Agency (IAEA). Nuclear forensics support. IAEA Nuclear Security Series No. 2-G (Rev. 1). Vienna: IAEA; 2019.
- Varga Z, Mayer K, Bonamici CE, Hubert A, Hutcheon I, Kinman W, et al. Validation of reference materials for uranium radiochronometry in the frame of nuclear forensic investigations. *Appl Radiat Isotopes*. 2015;102:81–86. <http://dx.doi.org/10.1016/j.apradiso.2015.05.005>
- Krajcók J, Varga Z, Yalcintas E, Wallenius E, Mayer K. Application of neodymium isotope ratio measurements for the origin assessment of uranium ore concentrates. *Talanta*. 2014;129:499–504. <http://dx.doi.org/10.1016/j.talanta.2014.06.02>



7. Brennecke GA, Borg LE, Hutcheon ID, Sharp MA, Anbar AD. Natural variations in uranium isotope ratios of uranium ore concentrates: Understanding the  $^{238}\text{U}/^{235}\text{U}$  fractionation mechanism. *Earth Planet Sci Lett.* 2010;291:228–233. <http://doi.org/10.1016/j.epsl.2010.01.023>
8. Švedkauskaitė-LeGore J. Development and validation of a method for origin determination of uranium-bearing material [PhD thesis report JRC-ITU-TN-2008/25]. Karlsruhe: European Union Joint Research Council, Institute of Transuranium Elements; 2008. Available from: <https://publications.jrc.ec.europa.eu/repository/handle/JRC44987>
9. Wallenius M, Mayer K, Ray I. Nuclear forensic investigations: Two case studies. *Forensic Sci Int.* 2006;156:55–62. <https://doi.org/10.1016/j.forsciint.2014.12.029>
10. Mathuthu M, Khumalo N. Developing nuclear forensics signatures and national nuclear forensics libraries for the African continent: A case review for South Africa. *Int J Appl Sci Res Rev.* 2017;4:1–3. <https://doi.org/10.21767/23949988.100052>
11. Keatley AC, Martin PG, Hallam KR, Payton OD, Awbery R, Carvalho F, et al. Source identification of uranium-containing materials at mine legacy sites in Portugal. *J Environ Radioact.* 2018;183:102–111. <https://doi.org/10.1016/j.jenvrad.2017.12.009>
12. IAEA Incident and Trafficking Database (ITDB). Incidents of nuclear and other radioactive material out of regulatory control [document on the Internet]. c2016 [cited 2019 Nov 04]. Available from: <http://wwwns.iaea.org/downloads/security/itdb-fact-sheet.pdf>
13. Keegan E, Kristo MJ, Colella M, Robel M, Williams R, Lindvall R, et al. Nuclear forensic analysis of an unknown uranium ore concentrate sample seized in a criminal investigation in Australia. *Forensic Sci Int.* 2014;240:111–121. <https://doi.org/10.1016/j.forsciint.2014.04.004>
14. Moody KJ, Hutcheon ID, Grant PM. Nuclear forensic analysis. 2nd ed. Boca Raton, FL: CRC Press; 2014.
15. Firestone RB, Shirley VS, Chu SYF, Balgoin CM, Zipkin J. Table of isotopes. CD ROM 8th ed. Version 1. Hoboken, NJ: Wiley-Interscience; 1996.
16. Scott SR, Sims KWW, Reagan MK, Ball L, Schwieters JB, Bouman C, et al. The application of abundance sensitivity filters to precise and accurate measurement of uranium series nuclides by plasma mass spectrometry. *Int J Mass Spect.* 2019;435:321–332. <https://doi.org/10.1016/j.ijms.2018.11.011>
17. Hutcheon I, Kristo M, Knight K. Non-proliferation nuclear forensics. Short course series #43 LLNLCONF-679869. Winnipeg: Mineralogical Association of Canada; 2015.
18. Maxwell O, Wagiran H, Ibrahim N, Lee SK, Sabri S. Comparison of activity concentration of  $^{238}\text{U}$ ,  $^{232}\text{Th}$  and  $^{40}\text{K}$  in different layers of subsurface structures in DeiDei and Kubwa, Abuja, north central Nigeria. *Radiat Phys Chem.* 2013;91:70–80. <http://dx.doi.org/10.1016/j.radphyschem.2013.05.006>
19. Spano TL, Simonetti A, Balboni E, Dorais C, Burns PC. Trace element and U isotope analysis of uraninite and ore concentrate: Applications for nuclear forensic investigations. *Appl Geochem.* 2017;84:277–285. <http://dx.doi.org/10.1016/j.apgeochem.2017.07.003>
20. Švedkauskaitė-LeGore J, Mayer K, Millet S, Nicholl A, Rasmussen G, Baltrunas D. Investigation of the isotopic composition of lead and of trace elements concentrations in natural uranium materials as a signature in nuclear forensics. *Radiochim Acta.* 2007;95:601–605. <https://doi.org/10.1524/ract.2007.95.10.601>
21. Richer S, Alonso A, De Bolle W, Wallum R, Taylor PDP. Isotopic “fingerprint” for natural uranium ore samples. *Int J Mass Spectrom.* 1999;193:9–14. [https://doi.org/10.1016/S1387-3806\(99\)00102-5](https://doi.org/10.1016/S1387-3806(99)00102-5)
22. Weyer S, Anbar AD, Gerdes A, Gordon GW, Algeo TJ, Boyle EA. Natural fractionation of  $^{238}\text{U}/^{235}\text{U}$ . *Geochim Cosmochim Acta.* 2008;72:345–359. <https://doi.org/10.1016/j.gca.2007.11.012>
23. Mishra S, Sahoo SK, Chaudhury P, Pradeepkumar KS. Measurement and validation of uranium isotope ratio in uranium ore for isotopic fingerprinting. *Radiat Prot Environ.* 2017;40:3–8. [https://doi.org/10.4103/rpe.RPE\\_36\\_16](https://doi.org/10.4103/rpe.RPE_36_16)
24. Bopp CJ, Lundstrom CC, Johnson TM, Glessner JJ. Variations in  $^{238}\text{U}/^{235}\text{U}$  in uranium ore deposits: Isotopic signatures of the U reduction process? *Geology.* 2009;37:611–614. <https://doi.org/10.1130/G25550A.1>
25. Bute SI. Uranium ore deposits in northeastern Nigeria: Geology and prospect. *Continent J Earth Sci.* 2013;8:21–28.
26. Tsang H, Akhtar S, Saif-ur-Rehman, Wu QF, Lee I, Sahir N, Yang XY. The uranium prospects in Mika Region, Northeastern Nigeria. *Open J Geol.* 2018;8:1043–1055. <https://doi.org/10.4236/ojg.2018.811063>
27. Martin RF, Bowen P. Per-aluminous granite produced by rock fluid interaction in the Riruwai non-orogenic ring complex, Nigeria: Mineralogical evidence. *Can Mineral.* 1981;19:65–82.
28. Olasehinde A, Ashano EC, Singh GP. Analysis of magnetic anomaly over the Riruwai Younger granite ring complex: A geodynamic implication. *Continent J Earth Sci.* 2012;7:9–18.
29. Nigeria Geological Survey Agency. Report on the integrated geophysical investigation of suspected base metal deposits in Kaffo part of Riruwai [document on the Internet]. No date [cited 2019 Dec 18]. Available from: <https://ngsa.gov.ng/author/ng-mod/page/3/>
30. Oruonye ED, Ahmed MY. Assessment of environmental effect of abandoned uranium mine site in Mika village of Taraba State Nigeria. *Int J Geog Geol.* 2017;6(4):70–78. <https://doi.org/10.18488/journal.10.2017.64.70.78>
31. Haruna AI, Ameh DP, Mohammed AA, Umar US. Uranium mineralisation in Gubrunde Horst, Upper Benue Trough, North-East, Nigeria. *J Geosci Geomat.* 2017;5(3):136–146. <https://doi.org/10.12691/jgg-5-3-5>
32. Suh CE, Dada SS. Mesosstructural and microstructural evidences for a two stage tectono-metallogenetic model for the uranium deposit at Mika, northeastern Nigeria: A research note. *Nonrenewable Resour.* 1998;7:75–77.
33. John SOO, Usman IT, Akpa TC, Ibrahim U. Rare earth elements in uranium ore for nuclear forensic application. *IOP Conf Ser Earth Environ Sci.* 2021;655, Art. #012075. <https://doi.org/10.1088/1755-1315/655/1/012075>
34. Almeida GM, Campos SSS, Gennari RF, Souza SO. Determination of the concentration of radionuclides in soil and water next the uranium mine of Caetité-ba. International Nuclear Atlantic Conference – INAC 2011; 2011 October 24–28; Belo Horizonte, Minas Gerais, Brazil. Associação Brasileira De Energia Nuclear; 2011.
35. Nicolet JP, Erdi-Krausz G. Guidelines for radioelement mapping using gamma ray spectrometry data. IAEA-TECDOC-1363. Vienna: International Atomic Energy Agency; 2003.
36. Tamborini G. SIMS analysis of uranium and actinides in microparticles of different origin. *Microchim Acta.* 2004;145:237–245. <http://doi.org/10.1007/s00604-003-0160-8>
37. Stirling CH, Anderson MB, Potter E-K, Halliday A. Low-temperature isotopic fractionation of uranium. *Earth Planet Sci Lett.* 2007;264:208–225. <https://doi.org/10.1016/j.epsl.2007.09.019>
38. Varga Z, Wallenius M, Mayer K, Mappen M. Analysis of uranium ore concentrates for origin assessment. *Proc Radiochem Acta.* 2011;1:1–4. <https://doi.org/10.1524/rcpr.2011.0004>
39. Fujii Y, Nomura M, Onitsuka H, Takeda K. Anomalous isotope fractionation in uranium enrichment process. *J Nucl Sci Technol.* 1989;26:1061–1064. <https://doi.org/10.1080/18811248.1989.9734427>
40. Morgenstern A, Apostolidis C, Mayer K. Age determination of highly enriched uranium: Separation and analysis of  $^{231}\text{Pa}$ . *Anal Chem.* 2002;74(21):5513–5516. <https://doi.org/10.1021/ac0203948>
41. Robin KH. Depleted uranium, natural uranium and other naturally occurring radioactive elements in Hawaiian environments. A report prepared for National Defence Centre for Environmental Excellence. Unpublished report; 2008.
42. Stanley FE. A beginner’s guide to uranium chronometry in nuclear forensics and safeguards. *J Anal At Spectrom.* 2012;27:1821–1830. <https://doi.org/10.1039/c2ja30182b>
43. Dalrymple GB. Age of the earth. Redwood City, CA: Stanford University Press; 1991.
44. Connelly JN, Bollard J, Bizzarro M. Pb-Pb chronometry and the early solar system. *Geochim Cosmochim Acta.* 2017;201:345–363. <http://dx.doi.org/10.1016/j.gca.2016.10.044>
45. Merle RE, Nemchin AA, Whitehouse MJ, Snape JF, Kenny GG, Bellucci JJ, et al. Pb-Pb ages and initial isotopic composition of lunar meteorites: NWA 773 clan, NWA 4734, and Dhofar 287. *Meteor Planet Sci.* 2020;55(8):1808–1832. <https://doi.org/10.1111/maps.13547>